Int J Clin Exp Pathol 2017;10(5):4927-4940
www.ijcep.com /ISSN:1936-2625/IJCEP0045775

Original Article

Hsa-miR-921 mediates lung injury via IL-37 in a rat model of traumatic hemorrhagic shock

Ying Zhang*, Qingming Lu*, Yan Lu, Zhaohui Li, Wen Chen, Xiaohua Xie

*Department of General Surgery of South Building, Chinese PLA General Hospital, Beijing 100853, China. *Co-first authors.*

Received November 27, 2016; Accepted February 17, 2017; Epub May 1, 2017; Published May 15, 2017

Abstract: Traumatic hemorrhagic shock (THS) is a serious and life-threatening complication of severe trauma that leads to acute lung injury; however, the detailed mechanism underlying THS remains unknown. Here, a rat THS model was established, involving the examination of interleukin (IL)-1 and IL-18 in serum; IL-1, IL-6, monocyte chemoattractant protein (MCP)-1, and keratinocyte chemoattractant (KC) in primary alveolar epithelial cells and alveolar macrophages; and the receptors for IL-1 and IL-18 (IL-1R and IL-18R, respectively) in primary alveolar macrophages. IL-37-regulated miRNAs were selected, identified by qRT-PCR, and validated using a dual-luciferase reporter gene assay. As expected, the expression of IL-1 and IL-18 was increased with prolonged trauma, peaking at 48 h, and was significantly decreased after hIL-37 treatment. Lung tissue was severely damaged with hyperemia of lung capillaries, and epithelial cell shedding, which was restored to normal after hIL-37 treatment. The ratio of wet to dry lung was significantly decreased after hIL-37 treatment, as well as the total protein measured in the bronchoalveolar lavage fluid (BALF) and fluorescein isothiocyanate (FITC)-dextran assay. Similarly, the expression of IL-1, IL-6, MCP-1, and KC in the lung, primary alveolar epithelial cells, and alveolar macrophages was significantly decreased after hIL-37 treatment, in addition to IL-1R and IL-18R in alveolar macrophages. The ratio of firefly luciferase/*Renilla* luciferase was significantly decreased, and indicated that hsa-miR-921 could bind the 3'-UTR of IL-37 to aggravate lung injury in the rat model of THS. These findings provided significant insight into the mechanism of lung trauma in THS, and uncovered hsa-miR-921, a novel potential IL-37 inhibitor.

Keywords: Traumatic hemorrhagic shock, lung trauma, inflammatory cytokine, miRNAs, IL-37

Introduction

Traumatic hemorrhagic shock (THS) is one of the most serious and life-threatening complications caused by severe trauma. It can lead to irreversible tissue injury in several organs despite immediate fluid resuscitation, and may result in death if not treated in time [1-3]. Acute lung injury (ALI) is a common complication of THS, and manifests as acute, progressive, and/or refractory hypoxemia, and may further develop into acute respiratory distress syndrome (ARDS) and multiple organ dysfunction syndrome (MODS) [3-6]. Following trauma, blood redistribution may induce intestinal tract ischemia that further damages the gastrointestinal mucosal barrier, which can induce bacterial translocation into the circulatory system, consequently inducing ALI [7-9]. The translocation of bacteria and their endotoxins initiates the immune system to activate thrombocytes and mononuclear-phagocytic cells that release a mass of inflammatory factors, such as tumor necrosis factor (TNF)-α, IL-1, IL-6, IL-8, platelet activating factor (PAF), and interferon (IFN)-γ [10-13]. When ALI occurs, microcirculation in the lung is blocked, tissues become hypoxic/ischemic, and alveolar epithelial cells are damaged [13, 14]. Importantly, when alveolar epithelial cells are damaged, some lung alveolar surfactants are reduced, vascular permeability is increased, and alveolus pulmonis is increased, which may induce edema in the lung and bleeding. When this occurs, ventilation and hemoperfusion become imbalanced and the oxygen supply is acutely decreased, which causes irreversible lung damage [5, 13, 15].

Interleukin-37 (IL-37) is a novel anti-inflammatory cytokine, involved in the regulation of both

innate and adaptive immunity, belonging to the IL-1 ligand family, and is associated with multiple immune diseases, such as the inhibition of innate immune responses, allergic dermatitis, and the inhibition of dendritic cell (DC) activation during intestinal inflammation. The A allele gene polymorphism of IL-37 (rs3811047) may be a defined element for rheumatoid arthritis. In peripheral blood mononuclear cells (PBMCs), macrophages, and epithelial cells, IL-37 is induced by a variety of pro-inflammatory cytokines, such as TNF-α, IL-1β, IL-8, IL-6, IFN-γ, and macrophage inflammatory protein (MIP)-2, and anti-inflammatory cytokines such as transforming growth factor (TGF)-β and IL-10, as well as toll-like receptors (TLR) [16-19]. In vivo, IL-37 is involved in complicated anti-inflammatory mechanisms that have not yet been elucidated. Several signaling pathways have been described, including the pathway that downregulates TLR-4/nuclear factor (NF)-κB signaling, the synergistic effect of IL-1β, and the binding of IL-1R8 and IL-18R to form IL-37-IL-1R8-IL-18Rα complexes [16, 19, 20]. In this study, we chose to explore the potential role of IL-37 in the prevention of THS, particularly with respect to the miRNAs that are involved in its regulation.

MicroRNAs (miRNAs) are endogenous noncoding small RNAs of 21-25 nucleotides, and are widely distributed in tissues and organs of different species. They have profound effects on their target genes by forming RNA-induced silencing complexes (RISCs) that partially bind to the 3' untranslated region (3'-UTR) of target genes to induce mRNA degradation or to inhibit mRNA translation. MiRNAs mainly regulate the physiology and development of tissues, and can induce changes in cell proliferation, cell cycle, apoptosis, cell migration and invasion, and angiogenesis. Altered miRNA expression could be a useful target for the early diagnosis and treatment of ALI, and may prove to be a significant biomarker and a novel therapeutic target.

Materials and methods

Animals and grouping

A total of 112 Sprague-Dawley rats (SD, male, SPF, 250-300 g) were purchased and raised in the Chinese PLA General Hospital Animal Center. They were housed at a temperature of 22 ± 1°C, in 40-50% humidity, in a 12-hr light/dark cycle. They were randomly divided into two groups: the hIgG group and the hIL-37 group. Within each group, seven time points were examined (0, 6, 12, 24, 48, 72, and 96 h), and eight rats were assessed at each time point. All animal experiments were approved by the Institutional Animal Care and Use Committee of the Chinese PLA General Hospital, and conformed to the current guidelines for the Care and Use of Laboratory Animals published by the U.S. National Institutes of Health (NIH Publication No. 85-23, revised 1996).

Establishment of rat traumatic hemorrhagic shock (THS) and treatment

The rat THS model was established based on an acute mechanical injury method as follows: after one week of adaptive feeding, rats were anesthetized with sodium pentobarbital (80 mg/kg, i.p.) and fixed. Subsequently, a No. 22 arteriovenous indwelling needle was used to perform the catheterization of the cervical artery and vein with heparin sodium (25 U/mL) anticoagulant, and blood pressure was monitored by a two-channel physiological recorder (type LMS2B) to stabilize the blood pressure between 80 and 100 mmHg. When the blood pressure was stabilized for 10 min at a minimum, the left leg was fixed on the chassis of a man-made bracket, and 300 g of iron was dropped from a height of 25 cm to cause a comminuted fracture in the middle section of the femur. After 30 min, artery intubation was performed and quick bleeding while simultaneously monitoring blood pressure. When blood pressure dropped to between 40 and 50 mmHg, and was maintained for 1 hr, rapid venous reinfusion was performed using twice the volume of liquids with a speed of 20 mL/hr, including autologous anticoagulated blood and ringer. The skin was sutured after disinfection and feeding was regulated. After modeling, 100 μL hIL-37 (10 μg/mL) or hIgG was intraperitoneally injected into the hIL-37 group and the hIgG group, respectively. After 48 hr, whole blood was collected from the eyes, the animals were sacrificed, and lung tissues were collected for further study.

Measurement of the lung weight ratio

The lung tissues were washed with 9% normal saline, and the wet weight of the lung was cal-

culated. Subsequently, the lung was dried in an oven at 80°C for 72 hr, and then the dry weight was calculated. Finally the weight ratio was calculated according to the following function: Weight ratio = (wet weight/dry weight) × 100%.

Measurement of lung permeability

After treatment with hIL-37, rats were fixed to expose the trachea, and 1 mL of phosphate buffered saline (PBS) was injected into the lung, and repeatedly beaten until swelling of the lung; the bronchoalveolar lavage fluid (BALF) was then collected to determine the total protein content.

In addition, 0.1 mL of FITC-labeled dextran (1 mg/mL) was injected into the tail vein for 2 hr, and rats were then sacrificed to potting PBS from the pulmonary artery. The lungs were then ground to tissue homogenate, and centrifuged at 4°C at 15,000 rpm for 30 min, and the supernatant was collected to obtain the absorbance value at 494 nm.

Measurement of IL-1 and IL-18 expression by enzyme-linked immunosorbent assay (ELISA)

Whole blood was incubated for 30 min at room temperature, and centrifuged at 4°C at 4,000 rpm for 10 min to obtain the serum. Subsequently, the serum IL-1 and IL-18 expression levels were detected using rat ELISA kits for IL-1 (ZKP-1604011, ZEKEBIO, Jiangsu, China) and IL-18 (ZKP-1604031, ZEKEBIO, Jiangsu, China) according to the manufacturer's instructions. After detection, data were recorded at 450 nm using a microplate reader for 15 min, and analyzed by SPSS software (version 21.0, http://spss.en.softonic.com/; Chicago, IL), and a histogram analysis was performed using Origin 9.5 software (http://www.originlab.com/).

Hematoxylin and eosin (HE) staining

Lung tissues were fixed and sectioned for HE staining as follows: slides were slightly overstained with hematoxylin for 3-5 min, and excess stain was removed with tap water. Slides were differentiated and destained for a few seconds in acidic alcohol until they appeared red. Then, the slides were briefly rinsed in tap water to remove the acid. Bicarbonate was applied for approximately 2 min, until the nuclei were distinctly visualized in blue. The hematoxylin-stained slides were placed in 70% ethanol after the final tap water rinse for 3 min and then in eosin for 2 min. Then, the slides were washed three times with 95% ethanol for 5 min, and were transferred to the first absolute ethanol of the clearing series. After staining, images were captured using a microscope connected to a CCD camera.

Measurement of the expression of IL-1, IL-6, MCP-1, and KC in the lung

Lung tissues were washed with 9% normal saline, and 20 μg was weighed, rapidly frozen in liquid nitrogen, homogenized with a grinder, and centrifuged at 5,000 rpm at 4°C for 10 min to collect the supernatant. Subsequently, the expression of IL-1, IL-6, MCP-1, and KC was measured using ELISA kits for rat IL-1 (ZKP-1604011, ZEKEBIO, Jiangsu, China), IL-6 (ZKP-1604013, ZEKEBIO, Jiangsu, China), MCP-1 (ZKP-1604023, ZEKEBIO, Jiangsu, China), and KC (ZKP-16040205, ZEKEBIO, Jiangsu, China) according to the manufacturer's instructions. After detection, data were recorded at 450 nm using a microplate reader for 15 min, and analyzed using SPSS software (version 21.0, http://spss.en.softonic.com/; Chicago, IL), and histogram analysis was performed using Origin 9.5 software (http://www.originlab.com/).

MiRNA extraction and quantitative reverse transcription-polymerase chain reaction (qRT-PCR) assay

Lung tissues were washed with 9% normal saline, and 20 μg was weighed, rapidly frozen in liquid nitrogen, homogenized with a grinder, and the miRNA was extracted using the miRcute miRNA extraction kit (DP501, TIANGEN Biotech (Beijing) CO., LTD, Beijing, China) according to the manufacturer's instructions. The concentration and the purity of miRNA were validated by ultraviolet spectrophotometry.

Subsequently, the extracted miRNA was used as a template in a reverse transcription reaction using a kit (TOYOBO, Japan) according to the manufacturer's instructions. The miRNA reverse transcription reaction mixture included 10 μL 2 × loading buffer, 1.2 μL miRNA RT primer/U6 small nuclear RNA primer, 2 μL miRNA template, 0.2 μL MMLV reverse transcriptase, and 6.6 μL DEPC-treated H_20. The reaction was

incubated at 26°C for 30 min, 42°C for 30 min, and 85°C for 10 min. For qRT-PCR, 100 ng cDNA was used as the template in the reaction mixture that included 10 μL 2 × Master Mix, 0.08 μL forward primer, 0.08 μL reverse primer, 2 μL cDNA template, 0.4 μL Taq DNA polymerase, and 7.44 μL ddH_2O. The qPCR amplification conditions were as follows: one cycle at 95°C for 3 min, 40 cycles at 95°C for 12 s, 62°C for 30 s, and 72°C for 30 s. The results were analyzed using the SDS 1.4 software (Applied Biosystems) based on 2-ΔΔCt, and histogram analysis using the Origin 9.5 software (http://www.originlab.com/).

Separation and culture of primary alveolar epithelial cells and alveolar macrophages

After modeling, rat lung was collected and infused five times each with 10 mL BALF I followed by 10 mL BALF II. Subsequently, a digestive juice containing 0.25% tryptase and 0.1% collagenase was infused into the lung, and digested for 30 min (refilled with digestive juice every 5 min), and the connective tissue was removed by sterile tweezers and scissors, and cut into pieces (1-2 mm^3). The tissues were then added to 5 mL cell dispersion liquid to halt digestion and transferred to a 37°C oscillator for 5 min at 150 rpm, then filtered using a 280-μM mesh sieve, centrifuged at 800 rpm for 10 min, and resuspended in Dulbecco's modified eagle medium (DMEM). The resuspended cells were seeded onto a rat IgG-coated plate, and centrifuged at 800 rpm for 10 min to remove the supernatant, and washed with serum-free DMEM. Finally, the cells were seeded at 1 × 10^6 cells/mL, incubated at 37°C with 5% CO_2 for 24 hr, transferred to DMEM, and incubated at 37°C with 5% CO_2.

Separation and culture of primary alveolar macrophages

After modeling, rat lung was collected and infused five times each with 10 mL BALF I followed by 10 mL BALF II. Subsequently, a digestive juice containing 0.25% tryptase and 0.1% collagenase was infused into the lung, and digested for 30 min (refilled with digestive juice every 5 min), and the connective tissue was removed by sterile tweezers and scissors, and cut to tissue pieces (1-2 mm^3). The tissues were then added to 5 mL cell dispersion liquid to halt digestion and then transferred to a 37°C oscillator for 5 min at 150 rpm, and then filtrated using a 280-μM mesh sieve, centrifuged at 800 rpm for 10 min, and resuspended in DMEM. The resuspended cells were seeded onto a rat IgG-coated plate, and centrifuged at 800 rpm for 10 min to remove the supernatant, and wished with serum-free DMEM. The cells were seeded at 1 × 10^6 cells/ml, and M-CSF (50 ng/ml) was added in each well; the cells were incubated in a CO_2-incubator with 5% CO_2 at 37°C for 48 hr, and then transferred to DMEM followed by incubation in a CO_2-incubator with 5% CO_2 at 37°C. After eight days, the cells were collected and analyzed by flow cytometry using the anti-rat F4/80 and anti-rat CD-11b antibodies.

Expression of IL-1, IL-6, MCP-1, and KC in primary alveolar epithelial cells and alveolar macrophages

The separated adherent primary rat alveolar epithelial cells and primary alveolar macrophages were washed with cold PBS three times, stimulated with hIL-37 and tissue homogenate for 24 hr, and the cell culture supernatant was collected to detect the change in expression of IL-1, IL-6, MCP-1, and KC using ELISA kits for rat IL-1 (ZKP-1604011, ZEKEBIO, Jiangsu, China), IL-6 (ZKP-1604013, ZEKEBIO, Jiangsu, China), MCP-1 (ZKP-1604033, ZEKEBIO, Jiangsu, China), and KC (ZKP-1604035, ZEKEBIO, Jiangsu, China) according to the manufacturer's instructions. After detection, data were recorded at 450 nm using a microplate reader for 15 min, and analyzed by SPSS software (version 21.0, http://spss.en.softonic.com/; Chicago, IL), and histogram analysis was performed using Origin 9.5 software (http://www.originlab.com/).

Western blot assay

The separated adherent rat primary alveolar macrophages were washed with cold PBS three times, stimulated with hIL-37 and tissue homogenate for 24 hr, and the total protein was measured using a BCA protein quantification kit (ZKP-C150045-1, Suzhou Zeke Biotech Co., LTD, China). Approximately 35 mg total protein was separated by electrophoresis on a 12.5% polyacrylamide gel, and transferred to a polyvinylidenedifluoride (PVDF) membrane (GE Healthcare) according to the manufacturer's instructions. The membrane was probed

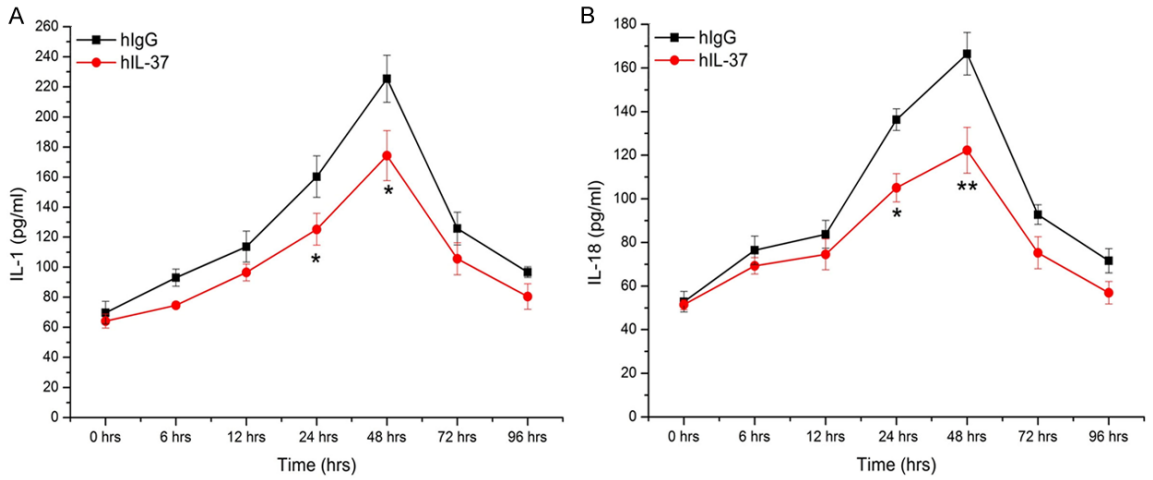

Figure 1. ELISA data depicting the expression of IL-1 (A) and IL-18 (B) in rat serum following prolonged trauma with hIL-37 treatment. Expression of both IL-1 and IL-18 steadily and significantly increased up to 48 hr, where it peaked, and then decreased until 96 hr (*P < 0.05, **P < 0.01, compared to hIgG group).

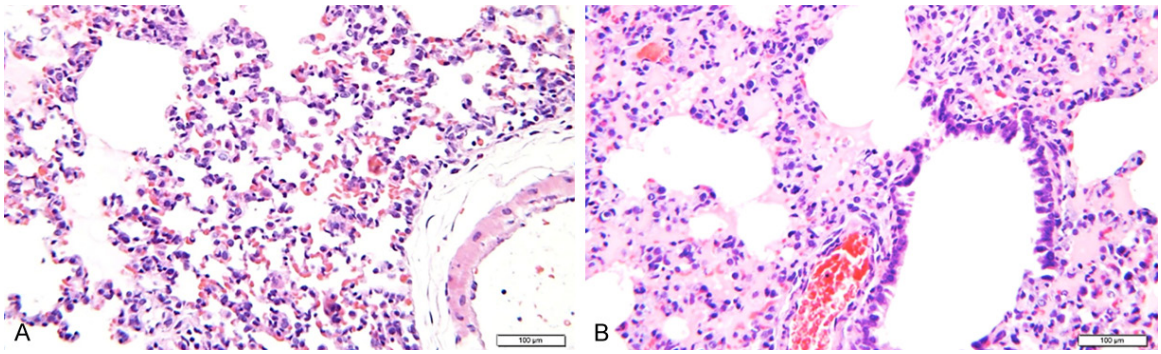

Figure 2. Histological examination of structural changes in the lung following trauma. A. A large number of red blood cells stranded in the capillaries, broadening of the alveolar septum, partial alveolar septum collapse, and effusion of neutrophils and fibrous protein were observed. B. After hIL-37 treatment, damage to the lung was alleviated.

with polyclonal primary antibodies anti-IL-18R (ab203191, Abcam, USA), anti-IL-1R8 (ab117480, Abcam, USA), and an anti-GAPDH monoclonal antibody (ab8245, Abcam, USA) for 1.5 hr at room temperature. The membrane was then incubated with a horseradish peroxidase-conjugated goat anti-mouse secondary antibody (1:5,000 in TBST; Beijing Golden Bridge Biotechnology Company Ltd, China) at room temperature for 1 hr. A chemiluminescence luminol reagent (ZKP-C150044-1, Suzhou Zeke Biotech Co., LTD, China) was used to develop the immune-labeled bands on an X-ray film, and the optical density of the bands was quantified using ImageJ 1.46 software (http://rsb.info.nih.gov/ij/download.html), and a histogram was generated using Origin 9.5 software (http://www.originlab.com/).

Bioinformatics analysis of hIL-37-regulated miRNAs

The list of human miRNAs was collected from the miRbase database (http://www.mirbase.org/), and the cross-talk miRNAs were screened based on the TargetScan database (http://www.targetscan.org/vert_71/), as well as the miRDB (http://www.mirdb.org/miRDB/) and miRanda (http://www.microrna.org/microrna/home.do) databases.

Construction of a dual-luciferase reporter-gene vector and assay

The miRNA sequences were obtained from the miRBase database, and the complementary single strand was designed and synthesized

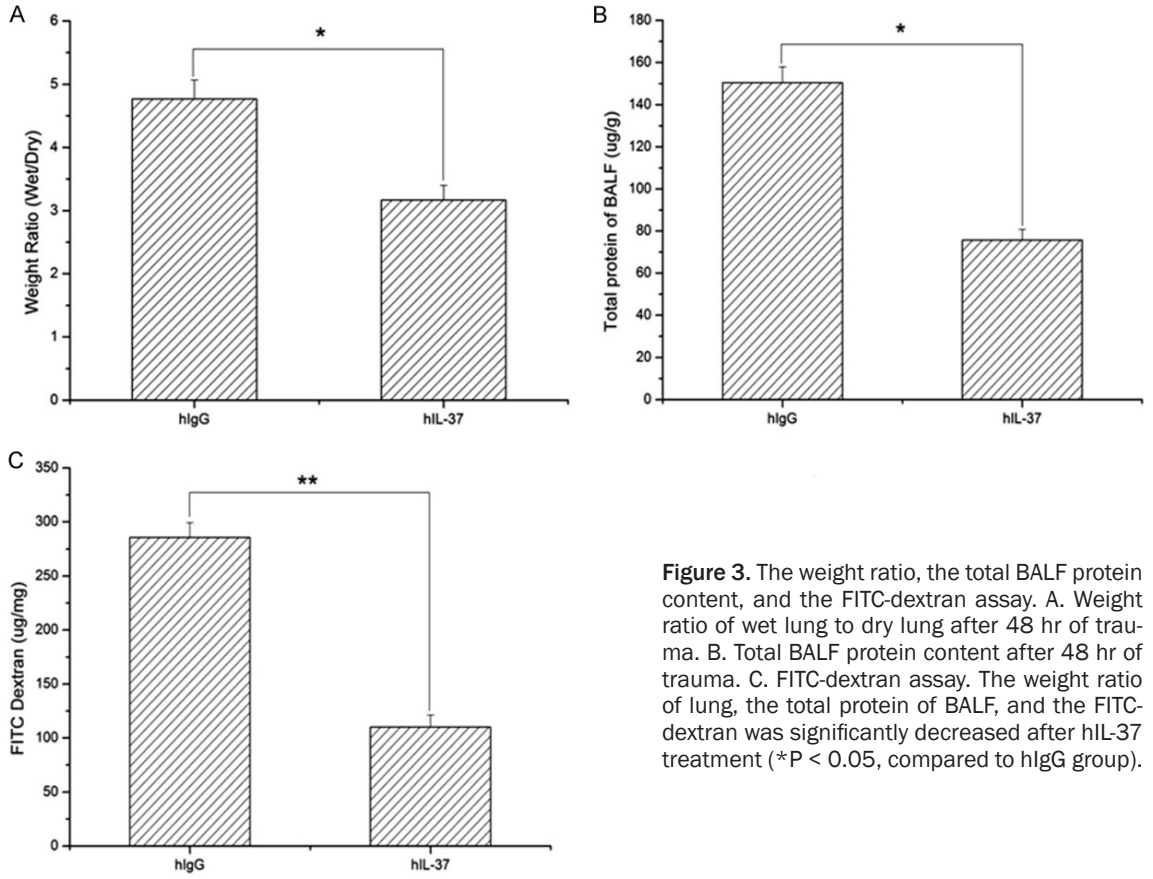

Figure 3. The weight ratio, the total BALF protein content, and the FITC-dextran assay. A. Weight ratio of wet lung to dry lung after 48 hr of trauma. B. Total BALF protein content after 48 hr of trauma. C. FITC-dextran assay. The weight ratio of lung, the total protein of BALF, and the FITC-dextran was significantly decreased after hIL-37 treatment (*P < 0.05, compared to hIgG group).

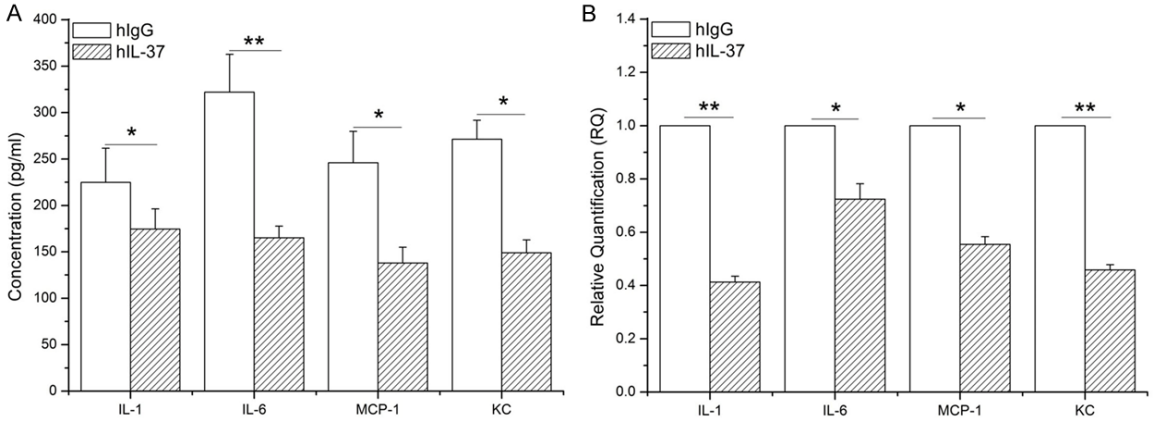

Figure 4. Expression of pro-inflammatory cytokines in the lung after hIL-37 treatment. A. ELISA was used to measure the protein expression of IL-1, IL-6, MCP-1, and KC in the lung following hIL-37 treatment. B. Quantitative RT-PCR was used to measure the mRNA expression of IL-1, IL-6, MCP-1, and KC in the lung after hIL-37 treatment. Both protein concentrations and mRNA expression of IL-1, IL-6, MCP-1, and KC were significantly decreased after hIL-37 treatment (*P < 0.05, compared to hIgG group).

for each miRNA. The full length 3'-UTR of the target gene was conjugated to sites for the restriction endonucleases EcoRI and XhoI (TaKaRa, Japan). After digestion with restriction enzymes, the target fragment was cloned into the psiCHECK-2 vector using T4 DNA ligase and was then used to transform competent *E. coli* DH5α cells (TaKaRa, Japan). A positive clone

Table 1. Primer sequences used for qRT-PCR in this study

Target gene	Primers sequences	
MCP-1	Forward	5'-AGGCAGATGCAGTTAATGCCC-3'
	Reverse	5'-ACACCTGCTGCTGGTGATTCTC-3'
KC	Forward	5'-GGCAGGGATTCACTTCAAGA-3'
	Reverse	5'-GCCATCGGTGCAATCTATCT-3'
IL-1	Forward	5'-TACCTATGTCTTGCCCGTGGAG-3'
	Reverse	5'-ATCATCCCACGAGTCACAGAGG-3'
IL-6	Forward	5'-GTCAACTCCATCTGCCCTTCAG-3'
	Reverse	5'-GGCAGTGGCTGTCAACAACAT-3'
GAPDH	Forward	5'-CCCCCAATGTATCCGTTGTG-3'
	Reverse	5'-TAGCCCAGGATGCCCTTTAGT-3'

was selected and plasmids were extracted for direct sequencing.

For the luciferase activity assay, 293T cells were plated 24 hr prior to transfection to obtain 30-50% confluence at the time of transfection, and were divided into four groups: Negative control (NC) + Wild type (WT), NC + Mutation (MUT), Mimic + WT, and Mimic + MUT. Fifty ng of the luciferase reporter plasmid were added to 100 μL Opti-MEM. Lipofectamine 2000 reagent was diluted 1:50 with Opti-MEM, incubated for 5 min, mixed with the mimic and the luciferase reporter plasmids, and incubated for 20 min. The cells were washed with serum-free medium, which was then discarded, and 800 μL of serum-free medium were added to each well. The mixture was gently added to each well for transfection at 37°C for 6 hr, and then replaced with fresh medium for an additional 48 hr. Cells were washed twice with PBS (3 min per wash), and the cells were then given a shock treatment by the addition of 100 μL 1 × PLB buffer followed by incubation at room temperature for 15 min. Twenty microliters of PLB lysis buffer was absorbed to a detector tube that already contained 100 μL Luciferase Assay Reagent II. Subsequently, 100 μL Stop&Glo reagent were added to detect the activity of the *Renilla* luciferase. The ratio of firefly luciferase/*Renilla* luciferase was calculated, and histogram analysis was carried out using Origin 9.5 software (http://www.originlab.com/).

Statistical analysis

All data are expressed as the mean ± standard deviation (SD). Statistical analysis was performed using one-way ANOVA using SPSS software (version 21.0, http://spss.en.softonic.com/; Chicago, IL), and Student's *t*-tests were performed in groups of two samples. $P < 0.05$ and $P < 0.01$ were considered significant and highly significant differences, respectively.

Results

Expression of IL-1 and IL-18 was significantly decreased in the lung after hIL-37 treatment

As exhibited in **Figure 1A** and **1B**, following trauma, hIgG and hIL-37 treatment resulted in a steady increase in the expression of IL-1 and IL-18 up to the 48-hr time point where it peaked. Expression then steadily decreased until the 96-hr time point. When compared to hIgG group, the expression of IL-1 and IL-18 in the hIL-37 group was significantly decreased at 24 hr and 48 hr following trauma (*$P < 0.05$, **$P < 0.01$).

Lung tissues were severely damaged after hIgG treatment, and restored to normal after hIL-37 treatment

As exhibited in **Figure 2A** and **2B**, HE staining demonstrated that a large number of red blood cells were stranded in the lung capillary, and there was obvious broadening of the alveolar septum, collapse of the partial alveolar septum, and effusion of neutrophils and fibrous protein. Following hIL-37 treatment, the lung damage was significantly alleviated and the tissue appeared to return to a normal state.

Weight ratio, total BALF protein, and FITC-dextran were significantly decreased after hIL-37 treatment

The weight ratio was significantly decreased following hIL-37 treatment when compared to hIgG treatment (**Figure 3A**, *$P < 0.05$). Similarly, hIL-37 treatment resulted in a significant reduction in the total BALF protein content (**Figure 3B**) as well as FITC-dextran (**Figure 3C**) when compared to hIgG treatment (*$P < 0.05$, **$P < 0.01$, respectively).

Expression of IL-1, IL-6, MCP-1, and KC in the lung was significantly decreased following hIL-37 treatment

When compared to the hIgG group, the expression of the inflammatory cytokines IL-1, IL-6,

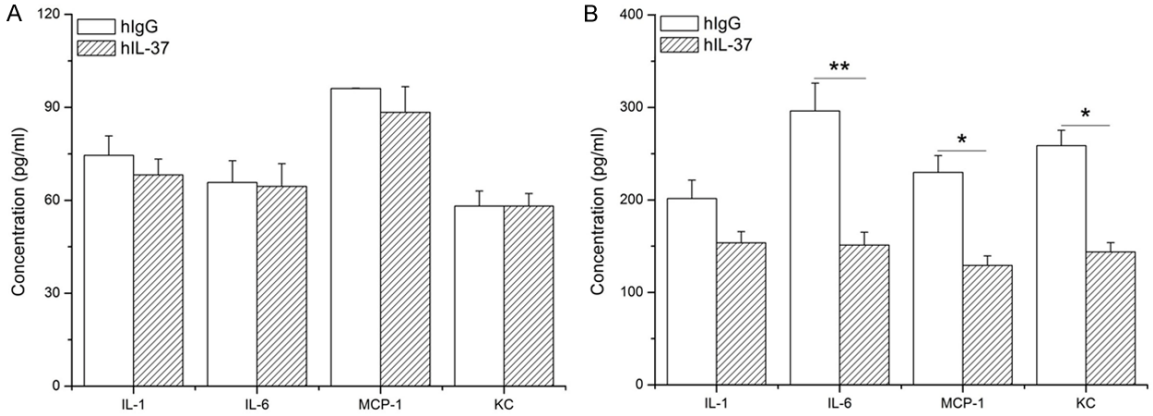

Figure 5. Expression of pro-inflammatory cytokines in primary alveolar epithelial cells and alveolar macrophages after hIL-37 treatment. ELISA was used to measure the protein expression of IL-1, IL-6, MCP-1, and KC after hIL-37 treatment. Expression of each cytokine was significantly reduced in (A) primary alveolar epithelial cells and in (B) alveolar macrophages after hIL-37 treatment (*P < 0.05, compared to hIgG group).

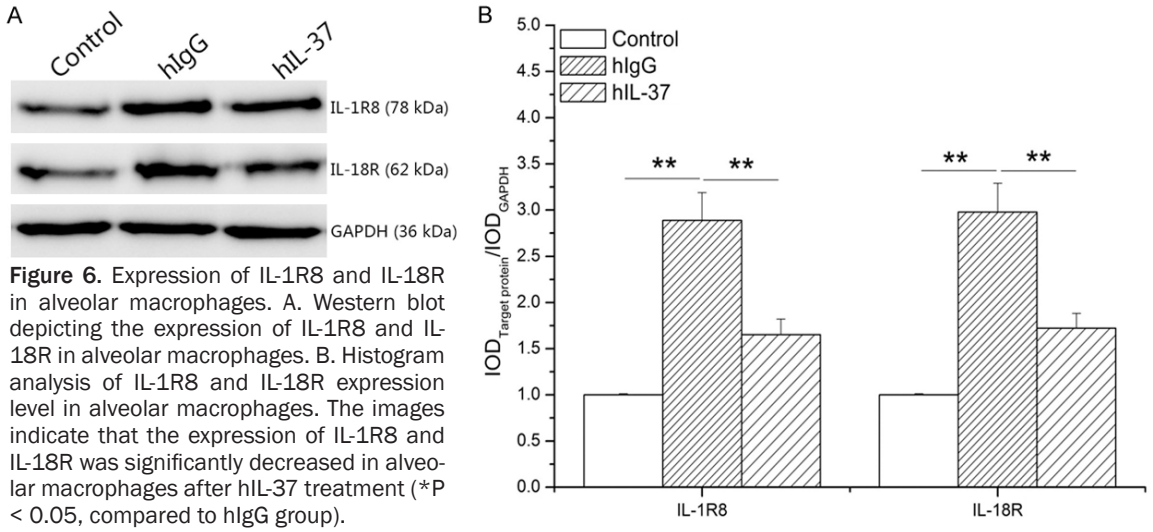

Figure 6. Expression of IL-1R8 and IL-18R in alveolar macrophages. A. Western blot depicting the expression of IL-1R8 and IL-18R in alveolar macrophages. B. Histogram analysis of IL-1R8 and IL-18R expression level in alveolar macrophages. The images indicate that the expression of IL-1R8 and IL-18R was significantly decreased in alveolar macrophages after hIL-37 treatment (*P < 0.05, compared to hIgG group).

MCP-1, and KC in the lung was significantly decreased after hIL-37 treatment (**Figure 4A**, *P < 0.05, **P < 0.01). Similarly, the mRNA expression of IL-1, IL-6, MCP-1, and KC in the lung exhibited the same trend, and was significantly decreased after hIL-37 treatment when compared to that after hIgG treatment (**Figure 4B**, *P < 0.05, **P < 0.01). The primers used are shown in **Table 1**.

Expression of IL-1, IL-6, MCP-1, and KC in primary alveolar epithelial cells and alveolar macrophages was significantly decreased after hIL-37 treatment

When compared to the hIgG group, the expression of the inflammatory cytokines IL-1, IL-6, MCP-1, and KC in alveolar macrophages was significantly decreased after hIL-37 treatment (**Figure 5B**, *P < 0.05, **P < 0.01); however, there were no significant differences between the treatment groups in the expression of IL-1, IL-6, MCP-1, and KC in alveolar macrophages (**Figure 5A**).

Expression of IL-1R8 and IL-18R was significantly decreased following hIL-37 treatment

The expression of IL-1R8 and IL-18R increased significantly following hIgG treatment when compared to that in the control (**P < 0.01), and significantly decreased following treatment with hIL-37, when compared to that in the hIgG group (**Figure 6A** and **6B**, **P < 0.01).

Table 2. IL-37-regulated miRNAs and their corresponding regulatory sites

miRNA family	Poorly conserved sites					Cumulative weighted context++ score	Total context++ score
	Total	8mer	7mer-m8	7mer-A1	6mer sites		
hsa-miR-921	1	1	0	0	0	-0.89	-0.89
hsa-let-7-3p	1	1	0	0	0	-0.63	-0.63
hsa-miR-4666-3p	1	1	0	0	0	-0.61	-0.61
hsa-miR-4694-5p	1	0	0	1	0	-0.44	-0.44
hsa-miR-657	1	0	1	0	0	-0.44	-0.44
hsa-miR-4468	1	0	0	1	0	-0.38	-0.38
hsa-miR-3606-5p	1	0	0	1	0	-0.37	-0.37
hsa-miR-4464	1	0	1	0	0	-0.36	-0.36
hsa-miR-4476-5p	1	0	1	0	0	-0.35	-0.35
hsa-miR-3174	1	0	0	1	0	-0.35	-0.35
hsa-miR-3591-5p	1	0	0	1	0	-0.33	-0.33
hsa-miR-5000-5p	1	0	0	1	0	-0.29	-0.29
hsa-let-7-3p	1	0	0	1	0	-0.28	-0.28
hsa-miR-7849-3p	1	0	0	1	0	-0.27	-0.27
hsa-miR-3671	1	0	0	1	0	-0.24	-0.24
hsa-miR-4789-5p	1	0	0	1	0	-0.16	-0.16
hsa-miR-607	1	0	1	0	0	-0.13	-0.13

Hsa-miR-921 expression was significantly decreased following hIL-37 treatment

To elucidate the change in IL-37-regulated miRNAs, several miRNAs were selected, as shown in **Table 2**, and qRT-PCR was performed using primers shown in **Table 3**. Of the miRNAs that were examined, hsa-miR-921 was significantly decreased following hIL-37 treatment (**Figure 7**, $^{**}P < 0.01$).

Hsa-miR-921 significantly down-regulated the expression of IL-37 by binding to its 3'-UTR

In a dual-luciferase reporter gene assay (**Figure 8**), after co-transfecting cells with hsa-miR-921 Mimic + WT (psiCHECK-2-UTR (IL-37)), the ratio of firefly luciferase/*Renilla* luciferase was significantly decreased ($^{**}P < 0.01$) when compared to that of NC + WT, NC + MUT and Mimic + MUT.

Discussion

In this study, a rat THS model was established, and 48 hr of trauma was validated as an optimal length of time based on the increase in expression of IL-1 and IL-18, changes in lung pathology, and expression of inflammatory cytokines, including IL-1, IL-6, MCP-1, and KC. The expression of these cytokines was significantly reduced in the lung as well as in primary alveolar epithelial cells and alveolar macrophages following hIL-37 treatment, which led to the prevention of THS. Bioinformatics analysis based on IL-37-regulated miRNAs and qRT-PCR demonstrated that hsa-miR-921 could bind to the 3'-UTR of IL-37 and down-regulate its expression. This indicated that hsa-miR-921 mediated the lung trauma via IL-37 in THS, and provided significant insight into a potential mechanism of THS prevention.

THS is one of the most serious and life-threatening complications in clinical settings. It may cause irreversible injury despite immediate fluid resuscitation, and it can result in death [1-3]. ALI is a common complication of THS, and manifests as acute, progressive and refractory hypoxemia [7, 8, 21]. ALI is one of the numerous severe illnesses defined as ARDS, with a mortality rate of 40-50%, which is often induced by bacterial or viral infection, or trauma-induced hemorrhage with large aggregates of inflammatory cells [3, 5, 22]. With excessive inflammatory cell aggregation, the inflammatory response is elevated to induce apoptosis of alveolar epithelial cells and rupture of alveolar capillaries. This leads to further lung malfunction and a series of anoxic complications, which when combined with the pathological features of the increasing

Table 3. Primer sequences used for qRT-PCR in this study

Name	Sequence of primers (5'→3')
hsa-miR-921-frs	ACACTCCAGCTGGGCTAGTGAGGGACAGAAC
hsa-miR-921-rvs	CTCAACTGGTGTCGTGGAGTCGGCAATTCAGTTGAGGAATCCTG
hsa-let-7a-3p-frs	ACACTCCAGCTGGGCTAGTGTGAGGTAGTAGGTT
hsa-let-7a-3p-rvs	CTCAACTGGTGTCGTGGAGTCGGCAATTCAGTTGAGAACTATAC
hsa-miR-4666-3p-frs	ACACTCCAGCTGGGCTAGTGCATACAATCTGAC
hsa-miR-4666-3p-rvs	CTCAACTGGTGTCGTGGAGTCGGCAATTCAGTTGAGAAATACAT
hsa-miR-4694-5p-frs	ACACTCCAGCTGGGCTAGTGAGGTGTTATCCTAT
hsa-miR-4694-5p-rvs	CTCAACTGGTGTCGTGGAGTCGGCAATTCAGTTGAGGCAAATGG
hsa-miR-657-frs	ACACTCCAGCTGGGCTAGTGGGCAGGTTCTCACCC
hsa-miR-657-rvs	CTCAACTGGTGTCGTGGAGTCGGCAATTCAGTTGAGCCTAGAGA
hsa-miR-4468-frs	ACACTCCAGCTGGGCTAGTGAGAGCAGAAG
hsa-miR-4468-rvs	CTCAACTGGTGTCGTGGAGTCGGCAATTCAGTTGAGATCTCATC
hsa-miR-3606-5p-frs	ACACTCCAGCTGGGCTAGTGTTAGTGAAGGCTA
hsa-miR-3606-5p-rvs	CTCAACTGGTGTCGTGGAGTCGGCAATTCAGTTGAGAATTAAAA
hsa-miR-4464-frs	ACACTCCAGCTGGGCTAGTGAAGGTTTGGATAG
hsa-miR-4464-rvs	CTCAACTGGTGTCGTGGAGTCGGCAATTCAGTTGAGTATTGCAT
hsa-miR-4476-5p-frs	ACACTCCAGCTGGGCTAGTGCAGGAAGGATTTAG
hsa-miR-4476-5p-rvs	CTCAACTGGTGTCGTGGAGTCGGCAATTCAGTTGAGGCCTGTCC
hsa-miR-3174-frs	ACACTCCAGCTGGGCTAGTGTAGTGAGTTAGAGAT
hsa-miR-3174-rvs	CTCAACTGGTGTCGTGGAGTCGGCAATTCAGTTGAGGGCTCTGC
hsa-miR-3591-5p-frs	ACACTCCAGCTGGGCTAGTGTTTAGTGTGATAATG
hsa-miR-3591-5p-rvs	CTCAACTGGTGTCGTGGAGTCGGCAATTCAGTTGAGTCAAACGC
hsa-miR-5000-5p-frs	ACACTCCAGCTGGGCTAGTGCAGTTCAGAAGTGT
hsa-miR-5000-5p-rvs	CTCAACTGGTGTCGTGGAGTCGGCAATTCAGTTGAGACTCAGGA
hsa-let-7d-5p-frs	ACACTCCAGCTGGGCTAGTGAGAGGTAGTAGGTT
hsa-let-7d-5p-rvs	CTCAACTGGTGTCGTGGAGTCGGCAATTCAGTTGAGAACTATGC
hsa-miR-7849-3p-frs	ACACTCCAGCTGGGCTAGTGGACAATTGTTGATC
hsa-miR-7849-3p-rvs	CTCAACTGGTGTCGTGGAGTCGGCAATTCAGTTGAGAGGCCCAA
hsa-miR-3671-frs	ACACTCCAGCTGGGCTAGTGATCAAATAAGGACT
hsa-miR-3671-rvs	CTCAACTGGTGTCGTGGAGTCGGCAATTCAGTTGAGTGCACACT
hsa-miR-4789-5p-frs	ACACTCCAGCTGGGCTAGTGGTATACACCTGATA
hsa-miR-4789-5p-rvs	CTCAACTGGTGTCGTGGAGTCGGCAATTCAGTTGAGCATACACA
hsa-miR-607-frs	ACACTCCAGCTGGGCTAGTGGTTCAAATCCAGA
hsa-miR-607-rvs	CTCAACTGGTGTCGTGGAGTCGGCAATTCAGTTGAGGTTATAGA
U6-frs	CTCGCTTCGGCAGCACA
U6-rvs	AACGCTTCACGAATTTGCGT

capillary endothelial cell injury and permeability, leads to the exudation of a mass of proteins and inflammatory cells [21, 23, 24].

Several studies have indicated neutrophil involvement in the inflammatory response of ALI [14, 25, 26]. Neutrophils exist in the blood and often in exudated tissues where they release free radicals, pro-inflammatory factors, and protein lyase that induce local tissue injury [9, 14]. Due to the lower perfusion pressure of lung capillaries and the length of the lower branch of blood vessels, neutrophils move slowly, make contact, adhere to endothelial cells, and aggregate in the lung, further increasing the pulmonary artery pressure. Meanwhile, neutrophils can release inflammatory mediators that damage the endothelial cells, further inducing capillary permeability, and increasing interstitial tissue edema and protein content, which leads to further lung injury [6, 27].

IL-1F7, first discovered by Kumar in 2000, was determined to be the seventh cytokine of the IL-1 family, and was then renamed IL-37 in 2010 [28-31]. It was derived from hematopoietic cells, and exhibited anti-inflammatory activity through a variety of pro-inflammatory cytokines. Furthermore, IL-37 has attracted increasing attention as a novel immunosuppressor owing to its ability to inhibit several immune system-associated illnesses [28, 32]. As shown in a previous study, IL-37 associates with IL-1R8 and IL-18R to form a IL-37-IL-1R8-IL-18R complex that regulates immune inflammation as well as the expression of IL-1 and IL-18 [28, 33]. IL-1 is mainly generated by monocytes, endotheliocytes, and neutrophils with α and β subtypes, and it can accelerate the inflammatory response to induce inflammatory lung injury [29]. IL-18 is mainly produced by macrophages for the subsequent pro-

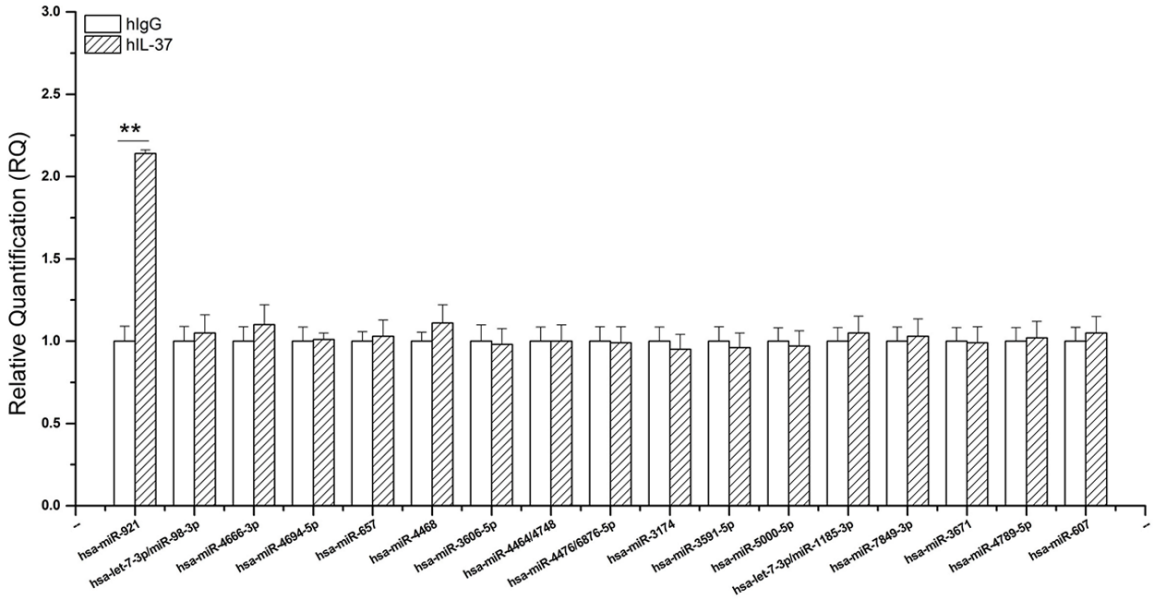

Figure 7. IL-37-regulated miRNAs identified by qRT-PCR. The expression of hsa-miR-921 was significantly increased following hIL-37 treatment (*P < 0.05, when compared to hIgG group).

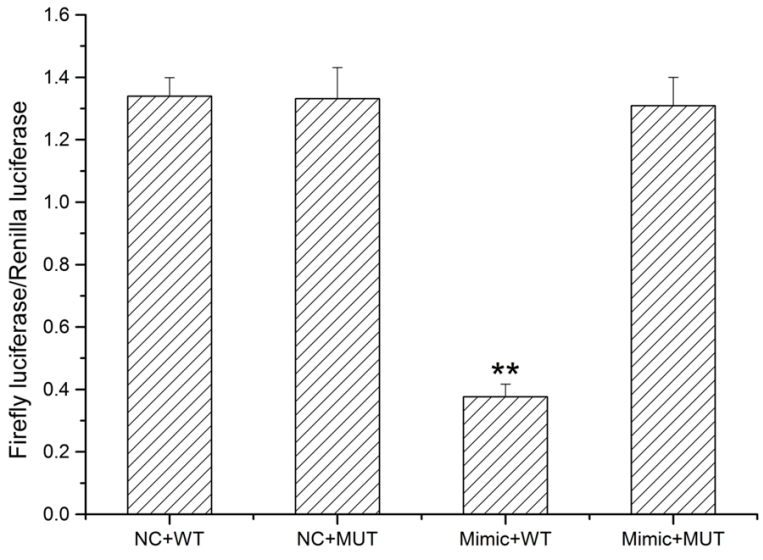

Figure 8. A dual-luciferase reporter gene assay depicting the regulation of hsa-miR-921 by the 3'-UTR of IL-37. Following co-transfection of the Mimic + WT, the ratio of firefly luciferase/*Renilla* luciferase was significantly decreased (**P < 0.01, compared to NC + WT, NC + MUT, and WT + MUT).

duction of IFN-γ, and to further activate and accelerate T cell secretion of IL-2, IL-4, and TNF-α [29].

In this study, a rat THS model was established, and after hIL-37 treatment, the expression of IL-1 and IL-18 was significantly increased 48 hr following trauma, where it peaked, and then decreased until the 96-hr time point. We, therefore, chose to study this 48-hr trauma time point further. In addition, after 48 hr of lung trauma with hIgG treatment, we observed rat lung capillary hyperemia, alveolar collapse, alveolar septa, neutrophil and fibrous protein exudation in the alveolar cavity, alveolar interval, bronchiole, and tracheal cavities, particularly alveolar cavity collapse and alveolar interval thickening. Following hIL-37 treatment, we observed alveolar interval broadening, less alveolar fibrous protein exudation, and a reduction in capillary hyperemia and epithelial cell apoptosis, indicating that hIL-37 could alleviate ATI-induce lung damage. The ratio of wet lung to dry lung reflected the degree of lung edema, and was significantly decreased following hIL-37 treatment when compared to that of the hIgG group, and indicated that IL-37 could alleviate the ATI-induced lung edema. In addition, the total BALF protein content reflected the exudation level of lung blood vessels or alveolar proteins,

and was significantly decreased following hIL-37 treatment when compared to that of the hIgG group, and indicated that IL-37 could alleviate the ATI-induced exudation of lung blood vessels or alveolar proteins. FITC-dextran is used as a permeability index, and reflects the alveolar capillary permeability. This index was significantly decreased following hIL-37 treatment when compared to that of the hIgG group, and indicated that IL-37 could decrease the alveolar capillary permeability that could, in turn, reduce the exudation of proteins and inflammatory cells. As demonstrated by ELISA, the expression of IL-1, IL-6, MCP-1, and KC was reduced in the ung tissue, primary alveolar epithelial cells, and alveolar macrophages following hIL-37 treatment, indicating that IL-37 could also decrease the expression of inflammatory cytokines to prevent the lung trauma associated with THS.

Several studies have demonstrated that miRNAs specifically regulate gene expression in cells to control a number of biological functions, including development, anti-viral defense, hematopoiesis, organ specificity, cell proliferation, apoptosis, fat metabolism, and cancer growth and development [34-36]. To elucidate the change in miRNAs after hIL-37 treatment, 17 IL-37-regulated miRNAs were screened initially, and hsa-miR-921 was found to be significantly increased. A dual-luciferase reporter gene assay demonstrated that the ratio of firefly luciferase/*Renilla* luciferase was significantly decreased in the Mimic + WT group, which indicated that the hsa-miR-921 mimic could bind to the 3'-UTR of IL-37, and further down-regulate its expression.

This study has few limitations, such as the limited number of samples and the limited number of miRNA targets. Future studies will focus on a detailed signaling pathway to reveal the protection of IL-37, and further explore a potential agent for intervention for the diagnosis and treatment of THS.

In conclusion, we report that we have established a rat model of THS, and have shown that IL-37 can prevent injury in this model. We have also demonstrated that hsa-miR-921 can bind the 3'-UTR of IL-37 and down-regulate its expression, which provides a potential approach to THS intervention in clinical settings, and also provides significant insight into the detailed mechanism underlying THS.

Acknowledgements

This work was supported by the "Twelfth Five-Year Plan" Key Scientific Research Foundation of PLA (BWS12J051).

Disclosure of conflict of interest

None.

Address correspondence to: Dr. Xiaohua Xie, Department of General Surgery, South Building, Chinese PLA General Hospital, 28 Fuxing Road, Beijing 100853, China. Tel: +86-10-66876364; Fax: +86-10-66876364; E-mail: n4xxh@126.com

References

[1] Beltran MJ, Becker TE, Hurley RK, Gurney JM and Hayda RA. Resuscitation and treatment of shock. J Orthop Trauma 2016; 30 Suppl 3: S2-S6.

[2] Leung LY, Deng-Bryant Y, Shear D and Tortella F. Experimental models combining TBI, hemorrhagic shock, and hypoxemia. Methods Mol Biol 2016; 1462: 445-458.

[3] Spinella PC, Perkins JG and Cap AP. Lessons learned for the resuscitation of traumatic hemorrhagic shock. US Army Med Dep J 2016; 37-42.

[4] Xanthos TT, Balkamou XA, Stroumpoulis KI, Pantazopoulos IN, Rokas GI, Agrogiannis GD, Troupis GT, Demestiha TD and Skandalakis PN. A model of hemorrhagic shock and acute lung injury in Landrace-Large White Swine. Comp Med 2011; 61: 158-162.

[5] Balkamou X, Xanthos T, Stroumpoulis K, Moutzouris DA, Rokas G, Agrogiannis G, Demestiha T, Patsouris E and Papadimitriou L. Hydroxyethyl starch 6% (130/0.4) ameliorates acute lung injury in swine hemorrhagic shock. Anesthesiology 2010; 113: 1092-1098.

[6] Lee C, Xu DZ, Feketeova E, Kannan KB, Yun JK, Deitch EA, Fekete Z, Livingston DH and Hauser CJ. Attenuation of shock-induced acute lung injury by sphingosine kinase inhibition. J Trauma 2004; 57: 955-960.

[7] Orowski T, Badowski A and Chabelski S. [Changes in the organs in hemorrhagic and traumatic shock]. Voen Med Zh 1977; 82-86.

[8] Pietra GG. The lung in shock. Hum Pathol 1974; 5: 121-122.

[9] Zambell KL, Phelan H, Vande Stouwe C, Zhang P, Shellito JE and Molina PE. Acute alcohol intoxication during hemorrhagic shock: impact

on host defense from infection. Alcohol Clin Exp Res 2004; 28: 635-642.
[10] Fischer H. [Current topics on shock. Review of literature]. MMW Munch Med Wochenschr 1976; 118: 1363-1370.
[11] Kriuk AS, Bazarevich GIa, Zeliak VI, Katkovskiĭ GB. [Acute respiratory failure in severe nonthoracic injury. The concept of the inflammatory nature of shock lung (a review of the literature and the authors' own data)]. Vestn Khir Im I I Grek 1984; 132: 135-140.
[12] Lee C, Xu DZ, Feketeova E, Nemeth Z, Kannan KB, Hasko G, Deitch EA and Hauser CJ. Calcium entry inhibition during resuscitation from shock attenuates inflammatory lung injury. Shock 2008; 30: 29-35.
[13] Murdock AD, Berseus O, Hervig T, Strandenes G and Lunde TH. Whole blood: the future of traumatic hemorrhagic shock resuscitation. Shock 2014; 41 Suppl 1: 62-69.
[14] Chen KB, Lee CY, Lee JJ, Tsai PS and Huang CJ. Platonin mitigates lung injury in a two-hit model of hemorrhage/resuscitation and endotoxemia in rats. J Trauma Acute Care Surg 2012; 72: 660-670.
[15] Bjerkvig CK, Strandenes G, Eliassen HS, Spinella PC, Fosse TK, Cap AP and Ward KR. "Blood failure" time to view blood as an organ: how oxygen debt contributes to blood failure and its implications for remote damage control resuscitation. Transfusion 2016; 56 Suppl 2: S182-189.
[16] Chen HM and Fujita M. IL-37: a new player in immune tolerance. Cytokine 2015; 72: 113-114.
[17] Ye Z, Wang C, Tang J, Zhou Y, Bai L, Liu Y, Kijlstra A and Yang P. Decreased interleukin-37 expression in Vogt-Koyanagi-Harada disease and upregulation following immunosuppressive treatment. J Interferon Cytokine Res 2015; 35: 265-272.
[18] Liu W, Deng L, Chen Y, Sun C, Wang J, Zhou L, Li H and Luo R. Anti-inflammatory effect of IL-37b in children with allergic rhinitis. Mediators Inflamm 2014; 2014: 746846.
[19] Dinarello CA and Bufler P. Interleukin-37. Semin Immunol 2013; 25: 466-468.
[20] Ding VA, Zhu Z, Xiao H, Wakefield MR, Bai Q and Fang Y. The role of IL-37 in cancer. Med Oncol 2016; 33: 68.
[21] Buhren V. [Pathophysiology of shock]. Unfallchirurg 1996; 99: 207-220.
[22] Bible LE, Pasupuleti LV, Gore AV, Sifri ZC, Kannan KB and Mohr AM. Chronic restraint stress after injury and shock is associated with persistent anemia despite prolonged elevation in erythropoietin levels. J Trauma Acute Care Surg 2015; 79: 91-96; discussion 96-97.
[23] Mathis KW, Zambell K, Olubadewo JO and Molina PE. Altered hemodynamic counter-regulation to hemorrhage by acute moderate alcohol intoxication. Shock 2006; 26: 55-61.
[24] Molina PE, Zambell KL, Norenberg K, Eason J, Phelan H, Zhang P, Stouwe CV, Carnal JW and Porreta C. Consequences of alcohol-induced early dysregulation of responses to trauma/hemorrhage. Alcohol 2004; 33: 217-227.
[25] Lee C, Xu DZ, Feketeova E, Kannan KB, Fekete Z, Deitch EA, Livingston DH and Hauser CJ. Store-operated calcium channel inhibition attenuates neutrophil function and postshock acute lung injury. J Trauma 2005; 59: 56-63; discussion 63.
[26] Sarin EL, Moore EE, Moore JB, Masuno T, Moore JL, Banerjee A and Silliman CC. Systemic neutrophil priming by lipid mediators in post-shock mesenteric lymph exists across species. J Trauma 2004; 57: 950-954.
[27] Xiang M, Fan J and Fan J. Association of Toll-like receptor signaling and reactive oxygen species: a potential therapeutic target for posttrauma acute lung injury. Mediators Inflamm 2010; 2010.
[28] Tete S, Tripodi D, Rosati M, Conti F, Maccauro G, Saggini A, Cianchetti E, Caraffa A, Antinolfi P, Toniato E, Castellani ML, Conti P and Theoharides TC. IL-37 (IL-1F7) the newest anti-inflammatory cytokine which suppresses immune responses and inflammation. Int J Immunopathol Pharmacol 2012; 25: 31-38.
[29] Boraschi D, Lucchesi D, Hainzl S, Leitner M, Maier E, Mangelberger D, Oostingh GJ, Pfaller T, Pixner C, Posselt G, Italiani P, Nold MF, Nold-Petry CA, Bufler P and Dinarello CA. IL-37: a new anti-inflammatory cytokine of the IL-1 family. Eur Cytokine Netw 2011; 22: 127-147.
[30] Pan F, Liao F, Xia G, Ge R, Mei Y, Tang X, Pan H, Ye D, Zou Y, Xu S and Xu J. Association of IL-1F7 gene with susceptibility to human leukocyte antigen-B27 positive ankylosing spondylitis in Han Chinese population. Clin Chim Acta 2010; 411: 124-126.
[31] Kumar S, Hanning CR, Brigham-Burke MR, Rieman DJ, Lehr R, Khandekar S, Kirkpatrick RB, Scott GF, Lee JC, Lynch FJ, Gao W, Gambotto A and Lotze MT. Interleukin-1F7B (IL-1H4/IL-1F7) is processed by caspase-1 and mature IL-1F7B binds to the IL-18 receptor but does not induce IFN-gamma production. Cytokine 2002; 18: 61-71.
[32] Gao W, Kumar S, Lotze MT, Hanning C, Robbins PD and Gambotto A. Innate immunity mediated by the cytokine IL-1 homologue 4 (IL-1H4/IL-1F7) induces IL-12-dependent adaptive and profound antitumor immunity. J Immunol 2003; 170: 107-113.
[33] Bufler P, Azam T, Gamboni-Robertson F, Reznikov LL, Kumar S, Dinarello CA and Kim SH. A complex of the IL-1 homologue IL-1F7b and IL-18-binding protein reduces IL-18 activi-

ty. Proc Natl Acad Sci U S A 2002; 99: 13723-13728.
[34] Kaviani M, Azarpira N, Karimi MH and Al-Abdullah I. The role of MicroRNAs in islet beta-cell development. Cell Biol Int 2016; 40: 1248-1255.
[35] Pinti MV, Hathaway QA and Hollander JM. Role of microRNA in metabolic shift during heart failure. Am J Physiol Heart Circ Physiol 2017; 312: H33-H45.
[36] Mohammadi M, Goodarzi M, Jaafari MR, Mirzaei HR and Mirzaei H. Circulating microRNA: a new candidate for diagnostic biomarker in neuroblastoma. Cancer Gene Ther 2016; 23: 371-372.